SHORELINE CHANGE AND LAND TRANSITIONS IN BHOLA ISLAND (1990–2025): A MULTI-DECADAL GIS-BASED ASSESSMENT

Hussain Muhammad Abdullah*[1], Kazi Md Ismail Hossain[2], SM Rifdu Rafee[3], Shariful Haque Sammo[4] and Al Rafi Islam[5]

[1] *Graduate, Mymensingh Engineering College, Bangladesh, e-mail: hmabdullah6670@gmail.com*
[2] *Graduate, Mymensingh Engineering College, Bangladesh, e-mail: kazimd.ismail787@gmail.com*
[3] *Graduate, Mymensingh Engineering College, Bangladesh, e-mail: rifduabd@gmail.com*
[4] *Graduate, Mymensingh Engineering College, Bangladesh, e-mail: sammohaque@gmail.com*
[5] *Graduate, Mymensingh Engineering College, Bangladesh, e-mail: alrafiislamrosin30@gmail.com*

ABSTRACT

This study comprehensively investigates the long-term and temporal dynamics of shoreline change on Bhola Island, Bangladesh, a highly vulnerable deltaic region within the Ganges-Brahmaputra-Meghna (GBM) Delta. The island, the largest in Bangladesh, has experienced significant land loss due to rapid erosional processes, which are exacerbated by heavy sediment flows, powerful tides, and storm surges. Understanding these dynamics is crucial for socio-economic sustainability, ecological stability, and infrastructure durability in the region (Caesar et al., 2015). The primary objective was to quantify shoreline movement and identify erosion and accretion patterns over a 35-year period (1990-2025) using multi-temporal satellite imagery. The methodology involved acquiring eight satellite images from USGS (Landsat 5 TM for 1990-2010 and Landsat 8 OLI/TIRS for 2015-2025). These images underwent rigorous pre-processing, including geometric, radiometric, and atmospheric corrections, to ensure accuracy and alignment with the Earth's true location. Shoreline extraction was performed using a semi-automatic method based on various water indexing transformations, including the Normalized Difference Water Index (NDWI), Modified Normalized Difference Water Index (MNDWI), and Automated Water Extraction Index (AWEI) variants(Tanvir Hassan et al., 2017). The Modified Normalized Difference Water Index (MNDWI) proved to be the most effective for representing the shoreline, exhibiting the minimum overlap distance in both Landsat and Sentinel imagery(Yılmaz et al., 2015; Toledo et al., 2024). Shoreline validation was conducted using Root Mean Square Error (RMSE) to compare extracted shorelines with real shoreline data and ground control points. Finally, shoreline change analysis was carried out using the QSCAT (QGIS Shoreline Change Analysis Tool) extension, employing statistical parameters such as Net Shoreline Movement (NSM), End Point Rate (EPR), and Linear Regression Rate (LRR) models(Manurung et al., 2025a). The study area was divided into three zones (Northern, Central, Southern Bhola) to better interpret geomorphological characteristics and erosion/accretion behavior. The analysis revealed significant & widespread erosion across Bhola Island. Over the long-term period (1990-2025), the average landward shoreline movement was approximately 12.85 meters per year, affecting 80.51% of the total transects analyzed. The highest erosion recorded was -4538.28 meters (or -36.31 m/year). While some localized accretion was observed, particularly in central sections, erosion remained the dominant trend, especially in the northern and southern zones. The time-series analysis, conducted at 5-year intervals, highlighted the episodic and non-linear nature of shoreline changes. Peak erosion events were recorded between 2000-2005 and 2015-2020, with some transects showing retreat exceeding 1600 meters in just five years. Conversely, accretion phases were observed in 1995-2000 and 2005-2010, suggesting periods of sediment build-up. The cumulative erosion area across the full time series was found to be significantly higher than the cumulative accretion area, underscoring the long-term vulnerability of Bhola's coast despite short-term gains. These findings emphasize that shoreline change in Bhola Island is a complex interplay of natural processes and human activities, necessitating adaptive coastal management strategies that can respond to both gradual & sudden shifts in shoreline position(Islam et al., 2015).

Keywords: *Shoreline change, Bhola Island, Erosion, Accretion, Satellite imagery, MNDWI*

1. INTRODUCTION

Deltaic coastlines are inherently dynamic systems, continuously reshaped by the interaction of river discharge, tidal currents, wave action, sediment transport, sea-level rise, and extreme events(Tanvir Hassan et al., n.d.). The Ganges–Brahmaputra–Meghna (GBM) delta represents one of the most active and vulnerable deltaic environments in the world, where low elevation, high population density, and frequent cyclones combine to intensify the impacts of shoreline instability. In such settings, coastal erosion is not only a geomorphic process but also a critical socio-environmental concern, directly affecting land resources, infrastructure, and livelihoods(Galib & Moniruzzaman, 2017).Bhola Island, located within the Meghna estuarine system at the southern margin of the GBM delta, occupies a particularly exposed position. Strong tidal currents, high sediment flux, and recurrent storm surges drive rapid and spatially uneven shoreline adjustments along its coast(Islam et al., 2015). Previous studies have documented erosion and accretion patterns in different parts of the delta; however, many are constrained by short temporal coverage, reliance on single change-rate indicators, or inconsistent shoreline extraction techniques, which limit the comparability and reproducibility of their results(Elahi, n.d.).

This study seeks to address these limitations by providing a consistent, multi-decadal assessment of shoreline dynamics of Bhola Island for the period 1990–2025 using an open-source GIS-based framework. Multi-temporal Landsat imagery is analyzed through a combination of spectral water indices and transect-based statistical measures, including Net Shoreline Movement (NSM), End Point Rate (EPR), and Linear Regression Rate (LRR), evaluated at a high confidence level(Manurung et al., 2025b). By integrating accuracy-tested shoreline delineation with uniform geometric and statistical treatment across all epochs, the study offers a more robust basis for identifying persistent erosion hotspots and temporal variability.The principal contribution of this work lies in its long-term, methodologically consistent, and reproducible approach to shoreline change analysis in a highly dynamic deltaic setting. Such an approach provides not only region-specific insights for Bhola Island but also a transferable framework for coastal monitoring and management in other erosion-prone sectors of the GBM delta and similar low-lying coastal systems.

1.1 Study Area

Bhola Island is the largest island of Bangladesh with an area of 1441 km2. Geographical coordinates of Bhola Island(lat.): 22° 41' 0" N (22.6833), (long.): 90° 39' 0" E (90.65). Most of the land area of Bhola

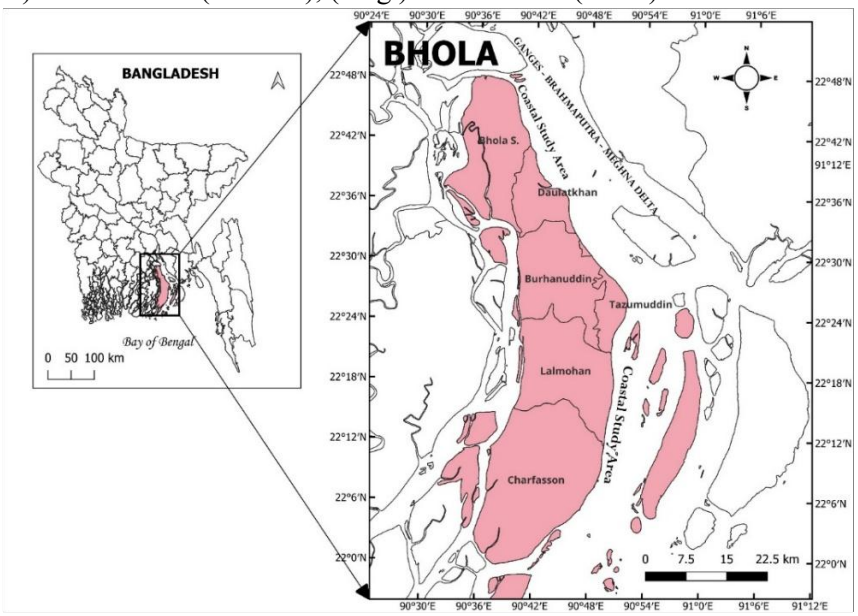

Figure 1. Location of Bhola Island within the Ganges–Brahmaputra–Meghna (GBM) delta, showing the study area in relation to major river systems and the Bay of Bengal.

District is under the administrative rule of Barisal Division. It is situated at the mouth of the Meghna River. The island is 130 kilometres (81 miles) long and has a population of 1.9 million. The shape of Bhola Island is elongated because of erosion by the Meghna River(Biswas & Islam, 2017).

Bhola Island sits in a region called the estuarine floodplain, where muddy rivers spill into the sea. Estuarine floodplains stay mostly flat, showing no twisting scars or old river channels, and their silty layers spread evenly in every direction, smooth as packed wet sand(Anwar & Rahman, 2021). A handful of narrow streams still wind through the area, but most of the old landscape drains through manmade canals that glint faintly where sunlight hits the water. You'll mostly find tidal creeks tracing the coastal edges of newer estuarine zones, where the water glints through the reeds (Brammer, 1996). Bhola Island's soil is calcareous alluvium, pale and fine like beach sand left behind after a tide. Seasonal floods and sluggish drainage leave the soil tasting faintly of salt. Fresh deposits of soil lie across the lower Meghna estuarine floodplain, their medium texture smooth underfoot and typical of the area (Brammer, 1996).

2. METHODOLOGY

2.1 Satellite Image Acquisition

We downloaded eight satellite images (Table 1) from the USGS Centre for Earth Resources Observation and Science at level 1 T, each one showing crisp details of land and water under clear skies All images were acquired at Level-1 terrain-corrected format with a nominal spatial resolution of 30 m. The shoreline change analysis can be broken into three main steps: first, clean and prep the images; next, pull out the shoreline itself; and finally, run the analysis like tracing that thin wet line where the waves just touched the sand(Bennett, 2021). To study how the shoreline shifted over time, multi-temporal satellite images were pulled from Landsat through the USGS Earth Explorer platform, using Landsat 5 TM for scenes from 1990 to 2010, a stretch of coast where the waves etched fresh lines in the sand each year. Landsat 8 OLI/TIRS was used for the years 2015 to 2025. Only cloud-free scenes (cloud cover <10%) were selected for accuracy.

2.2 Image Processing

Standard geometric, radiometric, and atmospheric pre-processing was applied to ensure spatial and spectral consistency across all images prior to shoreline extraction. Each Landsat image is offered as a Level 1TP product, where terrain distortions are corrected with a digital elevation model and precision is fine-tuned through an absolute adjustment using ground control points, the result as crisp and true as a pin. Radiometric correction removes pixel errors so each image looks cleaner, sharper, and free of faint colour distortions(Uddin et al., 2023). Radiometric correction involves calibrating the sensor data to turn raw Digital Numbers (DN) into radiance or reflectance values, then applying atmospheric correction to strip away the haze and reveal true surface reflectance. The Landsat and Sentinel images have already gone through radiometric correction, their tones balanced like light after a summer storm. Beyond those fixes, you also need atmospheric correction, since the pixel transformation depends on true surface reflectance, like how sunlight bounces off wet pavement after rain(Ahmed et al., 2018). Landsat and Sentinel images were corrected for the atmosphere in varying degrees, each using its own algorithm, one might sharpen the haze over a forest while another smooths the glare off a lake. Because Bhola Island stretches beyond one Landsat tile, we needed two overlapping scenes for each time point, like pieces of a puzzle fitting together along the muddy coast. In 2020, we used two Landsat 8 scenes:

- LO08_L1TP_137044_20201109_20201120_02_T1_B3_1
- LO08_L1TP_137045_20201109_20201120_02_T1_B3_1

and mosaicked them in QGIS to create a seamless image of the region, then trimmed that mosaic to Bhola Island's boundary for detailed analysis, the coastline faintly visible like a silver thread. We reprojected the final output to match the study area's coordinate reference system (EPSG 32646: WGS 1984 – UTM Zone 46 N), lining it up precisely with the map's grid(Rahman et al., n.d.).

2.3 Shoreline Extraction

Shorelines were extracted from multi-temporal Landsat imagery using a semi-automatic approach based on spectral water indices. The extraction focused on maintaining consistent delineation of the land–water boundary across all study years to support reliable long-term shoreline change analysis.

Several commonly used water indices were evaluated for shoreline delineation, including the Normalized Difference Water Index (NDWI), the Modified Normalized Difference Water Index (MNDWI), and Automated Water Extraction Index (AWEI) variants, based on their applicability to multispectral satellite imagery and coastal environments. Among these, MNDWI was selected for final shoreline extraction due to its superior performance in turbid, sediment-dominated deltaic environments and its ability to consistently separate water and land features along the Bhola Island coastline.

$$MNDWI = \frac{Green - SWIR1}{Green + SWIR2}$$

Table 1 presents the spectral band combinations used for water index computation for Landsat 5 TM, Landsat 8 OLI, and Sentinel-2 MSI imagery. The selected MNDWI raster outputs were reclassified into binary land–water surfaces to facilitate vector-based shoreline extraction(Rahman et al., n.d.).

Table 1. Band References

Sensor	Green Band	Blue Band	Red Band	NIR Band	SWIR1 Band	SWIR2 Band
Landsat 5 TM	Band 2	Band 1	Band 3	Band 4	Band 5	Band 7
Landsat 8 OLI	Band 3	Band 2	Band 4	Band 5	Band 6	Band 7
Sentinel-2 MSI	Band 4	Band 2	Band 4	Band 8	Band 11	Band 12

The classified raster images were first converted into polygon vector layers representing land and water bodies. These polygon features were subsequently transformed into line geometries using the QGIS Polygonize tool, from which the shoreline corresponding to the land–water interface was extracted. This vector-based approach ensured geometric consistency of shoreline positions and provided standardized shoreline line features suitable for subsequent validation and transect-based shoreline change analysis(Galib & Moniruzzaman, 2012).

2.4 Shoreline Validation and Digitization

Shoreline validation and digitization were carried out to assess the positional reliability of the extracted shorelines and to ensure geometric consistency across all study years. The shorelines derived from spectral water indices were evaluated using Root Mean Square Error (RMSE) by comparing satellite extracted shoreline positions with reference shoreline data and visually interpreted control points from high-resolution imagery. Given the 30 m spatial resolution of Landsat imagery, the positional uncertainty of the extracted shorelines is assumed to be within one pixel width, which is consistent with established shoreline change studies in deltaic and estuarine environments(Manurung et al., 2025b).

$$RMSE = \sqrt{\left[\frac{(residuals)^2}{number\ of\ transects\ intersected}\right]}$$

Following validation, the extracted shorelines were manually digitized using the Trace tool in QGIS to improve spatial continuity and reduce classification noise. Manual digitization was particularly important in complex geomorphological settings where tidal creeks, shallow water zones, and seasonal waterlogging can cause automated misclassification(Galib & Moniruzzaman, 2012). Digitization was performed at a consistent scale to maintain positional uniformity, and shoreline alignments were cross-checked against true colour Landsat imagery, Sentinel-2 images, and Google Earth visual interpretation.

Figure 2. Workflow of shoreline extraction showing conversion of MNDWI-derived raster output into polygon features and final shoreline line vectors using QGIS.

2.5 Shoreline Change Analysis

Shoreline change analysis was conducted using the QSCAT (QGIS Shoreline Change Analysis Tool), an extension of the open-source QGIS platform designed for transect-based shoreline assessment. A baseline was established parallel to the general orientation of the coastline, from which evenly spaced transects were generated perpendicular to the shoreline to intersect all extracted shoreline positions.

Net Shoreline Movement (NSM), End Point Rate (EPR), and Linear Regression Rate (LRR) were computed to quantify shoreline dynamics over time. NSM represents the cumulative displacement of the shoreline between the earliest and latest observation years, EPR provides average annual rates of shoreline change over defined temporal intervals, and LRR was used to evaluate long-term trends by fitting a regression line through all shoreline positions along each transect. The inclusion of multiple statistical indicators allows both absolute displacement and temporal variability in shoreline behavior to be captured. For the LRR analysis, shoreline change rates were evaluated at a 99.7% confidence level, following the default statistical implementation of the QSCAT framework adapted from DSAS. Shoreline change statistics were analyzed for erosion and accretion trends across eight time intervals spanning the period 1990–2025, enabling assessment of both long-term shoreline evolution and intermediate-scale variability(Manurung et al., 2025b).

3. RESULTS & DISCUSSIONS

3.1 Shoreline Extraction and Validation

MNDWI performed the best in representing the shoreline both in Landsat and Sentinel as shown in Table 2, as the minimum overlap distance was from MNDWI and followed by AWEI SH. MNDWI and AWEI were good at detecting mixed pixels that represent small ponds and rivers, MNDWI performed the best for extracting water bodies. Based on this, all shorelines used in the next analysis are obtained with MNDWI index.

Table 2. RMSE value of shoreline with different indices transformation

Index	RMSE with Baseline 2020 (m)		RMSE with Google Earth GCP (m)	
	Landsat 2020	Sentinel 2020	Landsat 2025	Sentinel 2025
MNDWI	90.44545	101.36128	42.47452	23.54781
NDWI	130.62547	143.61752	64.92843	41.75624

AWEI NSH	-	124.21764	-	32.91542
AWEI SH	92.65328	103.57143	46.69964	26.58145

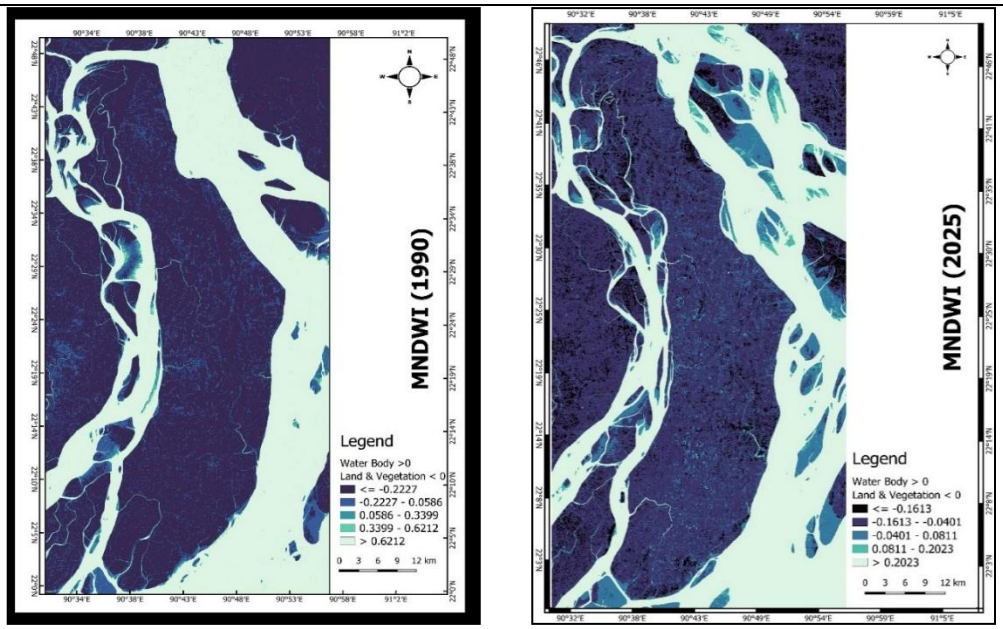

Figure 3. MNDWI-derived shoreline representation for Bhola Island in 1990 and 2025, illustrating long-term changes in the land–water boundary.

3.2 Shoreline Change

Figure 3 illustrates the spatial and temporal dynamics of shoreline change along the eastern coastline of Bhola Island between 1990 and 2025, using extracted shorelines at 5-year intervals. The shoreline positions were derived from satellite imagery using the MNDWI index in GIS, and were analyzed in QGIS using the QSCAT extension for systematic shoreline change detection. To better interpret the patterns, the study area was divided into three zones (Zone 1, Zone 2, and Zone 3) based on geomorphological characteristics and visible erosion/accretion behavior.

Zone 1 (Northern Bhola): Displays noticeable landward retreat of the shoreline from 1990 to 2025. High variability in shoreline positions indicates unstable erosion dynamics, likely influenced by tidal creeks and sediment redistribution. Shoreline movement appears more aggressive post-2010, aligning with known regional cyclone activity.

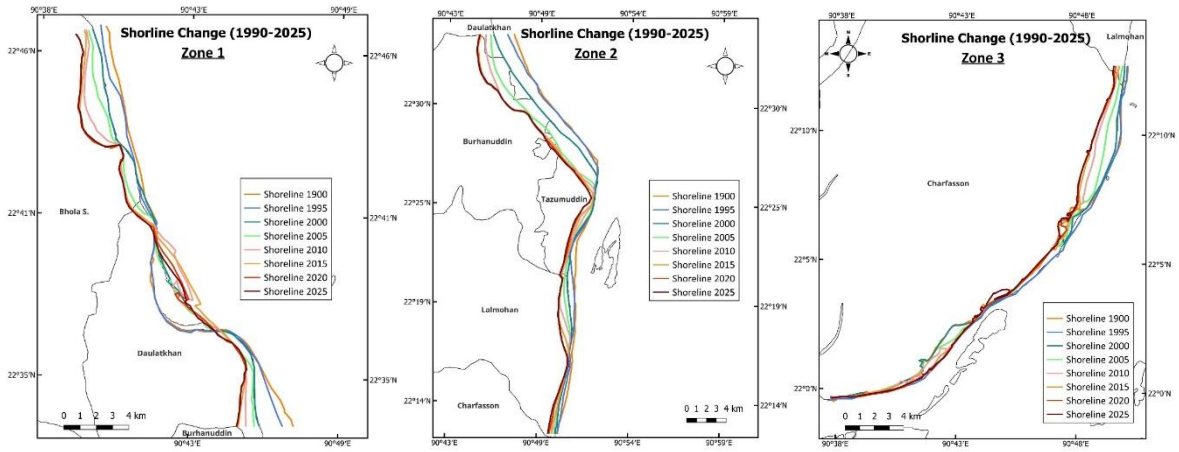

Figure 4. Multi-temporal shoreline positions at 5-year intervals (1990–2025) for Zone 1 (Northern Bhola), Zone 2 (Central Bhola), and Zone 3 (Southern Bhola), illustrating spatial variability in erosion and accretion patterns.

Zone 2 (Central Bhola): Shows a mix of erosion and localized accretion. Shorelines from 1995 to 2025 gradually migrate landward, but at a slower rate compared to Zone 1. Some stabilization is observed around 2015–2020, possibly due to localized protection structures or sediment rebalancing.

Zone 3 (Southern Bhola): This zone demonstrates progressive and consistent erosion, with shoreline retreat evident across all time slices. The shorelines in 2020 and 2025 are significantly offset from earlier years, suggesting accelerated land loss in recent decades. Proximity to tidal inlets and absence of significant protective structures may have contributed to this trend. The closely spaced shoreline contours highlight the intensity and continuity of coastal erosion, particularly in Zones 1 and 3.

Conversely, wider spacing between lines in certain segments reflects temporary accretion or slower erosion. This map confirms that shoreline change in Bhola Island is nonlinear, spatially variable, and influenced by both natural dynamics and anthropogenic pressures.

3.3 Shoreline Change Analysis

To comprehensively assess the spatial and temporal dynamics of shoreline change along Bhola Island, the QSCAT statistical module was employed. This tool allows for the quantitative measurement of shoreline movement over time by calculating statistical parameters such as Net Shoreline Movement (NSM), End Point Rate (EPR), and other change metrics along a series of evenly spaced transects(Manurung et al., 2025a). Shoreline positions, extracted from MNDWI-derived vector layers for multiple years, were input into QSCAT to produce two distinct temporal analyses:

3.3.1 Case 1 - Long-term analysis (1990-2025)

In this scenario, the shoreline change was assessed over the entire 35-year period (1990 to 2025) as a single interval. This allowed for a cumulative measurement of long-term erosion and accretion trends using NSM (Net Shoreline Movement) and EPR (End Point Rate). The outputs show the change, effectively capturing the total land loss or gain without interruption. This highlights overall erosion/accretion magnitude. Suitable for understanding general coastal retreat of advancement trends but misses intermediate fluctuations, such as temporary accretion or erosion events(Daud et al., 2021a).

Table 3. Value of shifting computed using NSM, EPR and LRR model from 1990 to 2025.

Shoreline Change rate	NSM (m)	EPR (m/year)	LRR (m/year)
Highest Erosion	-4538.28	-36.31	-35.49
Highest Accretion	1878.36	15.03	16.02
Average Shifting	-1178.97	-9.43	-8.96
Eroding:			
Total transects	1734	1727	1710
(%) transects	80.84	80.51	79.72
Average Erosion	-1600.32	-12.85	-12.49
Accreting:			
Total transects	392	388	435
(%) transects	18.28	18.09	20.28
Average Accretion	627.44	5.07	4.94

Graph 1 presents a summary of the change analysis results obtained using the EPR and LRR models for long term periods of observation. In the long-term analysis, EPR values along the transects indicate a maximum landward shoreline movement of 36.31 meters/year, and mean rate is 12.85 meters/year observed in 80.51% of total transects applied. Meanwhile, the average seaward movement is 5.07 meters/year, affecting 18.09% of the transects, with a maximum value of 15.03 meters per year. According to EPR, accretion is the dominant process, as reflected in the average shoreline shift of -9.43 m/year (a negative value indicating erosion). This finding is further supported by the NSM calculation, which confirms that accretion is the prevailing trend in the long-term dataset. Based on the LRR model, approximately 20.28% of the transects in this study indicate land accretion, with mean value is around

4.94m/year, while erosion is 35.5 m/year. Overall, the results highlight that erosion dominates, with a shoreline displacement of around 9.43 m/year. To account for uncertainty, LRR applies a 99.7% confidence interval (LCI)(Manurung et al., 2025a).

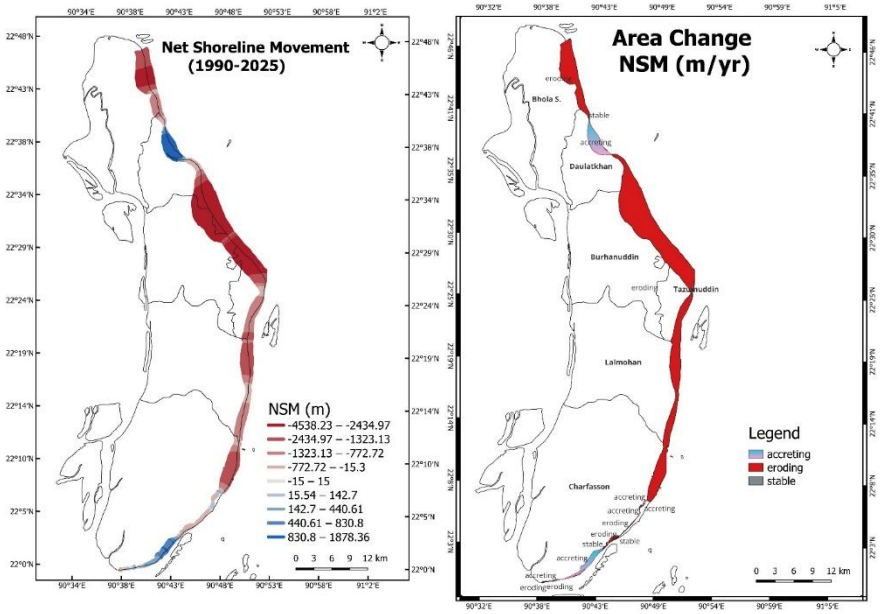

Figure 5. Spatial distribution of Net Shoreline Movement (NSM) along Bhola Island (left) and corresponding erosion–accretion area changes (right) for the 1990–2025 period.

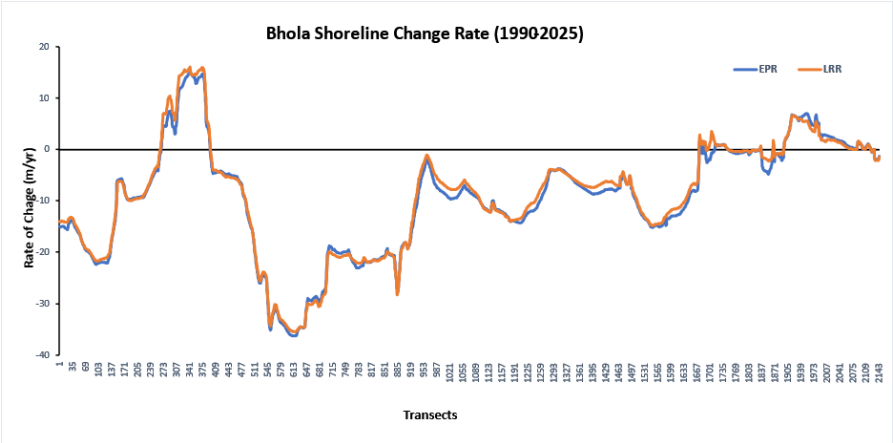

Graph 1. Distribution of End Point Rate (EPR) and Linear Regression Rate (LRR) values along shoreline transects for the long-term period (1990–2025).

3.3.2 Case 2 - Time Series with 5-Year Intervals (1990-2025)

In this case, the same shoreline data was analyzed in 5-year intervals (e.g., 1990-1995, 1995-2000, …, 2000-2025) to assess dynamic shoreline behavior over time. The QSCAT output for this case shows variable rates of erosion and accretion, reflecting the temporal instability of shoreline changes. The temporal resolution (5-year intervals) enhances the ability to detect episodic shifts, helping identify critical periods where erosion control interventions may have failed or succeeded.This reveals short-term shoreline behavior and cyclical patterns. It identifies specific period of intensified erosion, often aligned with major cyclonic event or human interventions but more complex to interpret due to fluctuating rates(Islam et al., 2015). The NSM results from the 5-year interval analysis reveal a high degree of spatial and temporal variability. Certain transects displayed alternating patterns of erosion and accretion over successive intervals, indicating dynamic coastal processes. Peak erosion events were recorded in intervals 2000–2005 and 2015–2020, with several transects showing NSM retreat exceeding

1600 m in just five years. Accretion phases were observed most notably in 1995–2000 and 2005–2010, suggesting periods of sediment build-up, possibly from upstream sediment influx or calmer hydrodynamic conditions. The data show that erosion dominates in the northern and southern zones during most intervals, while accretion tends to be localized in central sections.

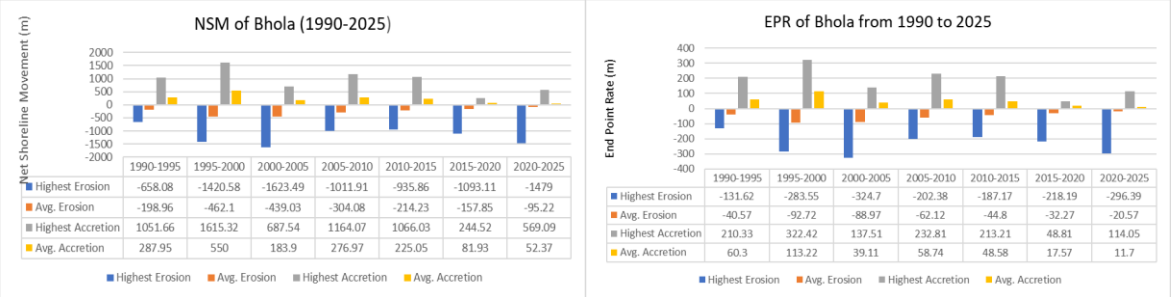

Graph 2. Temporal variation of NSM and EPR values computed at 5-year intervals (1990–2025), highlighting episodic shoreline erosion and accretion trends.

Although EPR is traditionally more suited for long-term comparisons, in this case it was calculated for each 5-year segment to better understand annualized rates of shoreline change over shorter timeframes. Maximum short-term erosion rates exceeded –10 m/year in the southern sector during 2015–2020, coinciding with the period following Cyclone Roanu (2016) and Cyclone Amphan (2020)(Rahman et al., n.d.). Short-term accretion rates reached up to +8 m/year in specific transects during 1995–2000, likely due to favorable tidal and sediment transport conditions(Daud et al., 2021b).

The erosion–accretion area chart for the 5-year interval analysis highlights episodic sediment redistribution. The largest net erosion occurred between 2000–2005, with erosion area exceeding accretion by over 37.79 km². The interval 1990–1995 displayed the highest net accretion. Across the full time series, the cumulative erosion area remains significantly higher than the cumulative accretion area, underscoring the long-term vulnerability of Bhola's coast despite short-term gains.

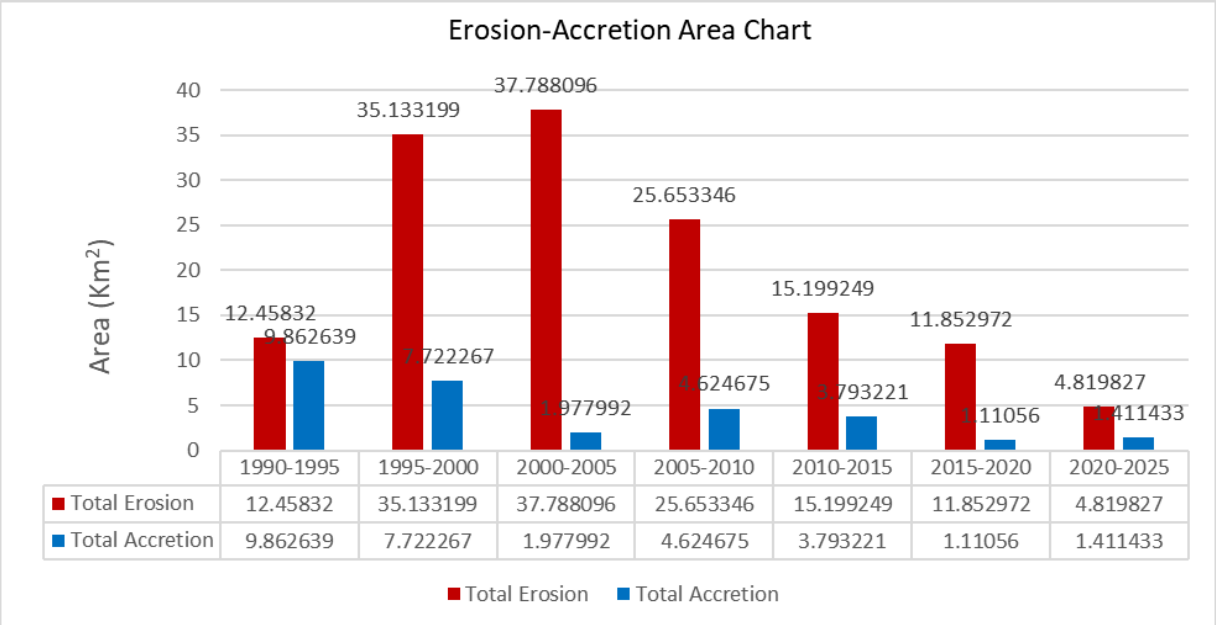

Graph 3. Comparison of erosion and accretion areas for Bhola Island across successive 5-year intervals, indicating periods of dominant land loss and gain.

This time-series analysis confirms that shoreline change in Bhola Island is non-linear and episodic, driven by the interplay of natural processes and human activities. While certain intervals showed short-lived accretion, these gains were often offset by severe erosion in subsequent periods. Such findings

emphasize the importance of adaptive coastal management strategies that can respond to both gradual and sudden changes in shoreline position(Daud et al., 2021a).

3.4 Uncertainty and Limitations

Despite the robustness of the multi-temporal GIS-based approach, several sources of uncertainty should be acknowledged when interpreting the shoreline change results. Positional uncertainty arises primarily from the 30 m spatial resolution of Landsat imagery, which constrains the precision of shoreline delineation to approximately one pixel width. Additional uncertainty is introduced by tidal stage variability at the time of satellite acquisition, as the extracted shorelines represent instantaneous waterlines rather than datum-referenced coastlines(Golam et al., n.d.). In complex deltaic environments such as Bhola Island, shoreline delineation errors may also occur due to turbid water conditions, shallow nearshore bathymetry, and mixed land–water pixels along tidal creeks and mudflats. While these factors can influence short-term shoreline position, the long-term, multi-decadal analysis employed in this study reduces the impact of individual image-level uncertainties on overall trend interpretation(Bennett, 2021).

4. CONCLUSION

This study provides a comprehensive, multi-decadal assessment of shoreline dynamics on Bhola Island from 1990 to 2025 using a fully GIS-based analytical framework. By applying AWEI-SH and MNDWI for shoreline extraction and computing NSM, EPR, and LRR metrics with QScat, the analysis reveals that coastal erosion is widespread, persistent, and spatially concentrated along the eastern and southern margins of the island. The highest erosion rates reached ≈36.31 m/year, while the maximum accretion was comparatively lower at ≈16.02 m/year, indicating a clear dominance of land loss over land gain. These patterns are reinforced by the observed long-term retreat of more than 1 km in certain transects, confirming that erosion on Bhola is both severe and sustained. Parallel LULC observations show a decline in vegetated/agricultural lands, expansion of waterlogged and tidal zones, and gradual growth of built-up areas, pointing to the weakening of the island's natural protective buffers. When contextualized with regional sea-level rise (≈3–4 mm/year) and repeated cyclone landfall exposure, it becomes evident that Bhola's erosion is being shaped by both chronic slow-onset processes and acute extreme events. The convergence of erosion, vegetation loss, and settlement growth in low-elevation, hazard-prone zones signals increasing socio-environmental vulnerability.

Overall, the study demonstrates that Bhola Island is undergoing progressive coastal reconfiguration, and that passive monitoring or isolated structural interventions are no longer adequate. A shift toward integrated and adaptive shoreline management is required.

Recommendations:

1. Immediate Intervention in Identified Hotspots: Priority should be given to the southern and southeastern coastal belts, particularly in Daulatkhan, Burhanuddin, and Monpura, where erosion intensity and human vulnerability are highest(Durap & Balas, 2024).

2. Adopt Hybrid Coastal Protection Strategies: Measures should incorporate both nature-based components (e.g., mangrove rehabilitation, saltmarsh expansion, sediment trapping) and low-impact structural elements (e.g., permeable breakwaters, geotextile dunes) rather than fully hard engineered structures(Almarshed et al., 2020; Durap & Balas, 2024).

3. Restore and Expand Vegetation Buffers: Reestablishing mangrove belts in suitable NDVI-supported zones will enhance sediment stabilization and reduce wave energy naturally(Toledo et al., 2024).

4. Local Monitoring and Data Strengthening: Establish regular shoreline monitoring using drones, GNSS surveys, and tide-gauge calibration to reduce dependence on remote-only data and to improve the reliability of future modeling efforts(Durap & Balas, 2024).

5. Community-based Planning and Protection: Engage local stakeholders in planning, land-use regulation, and managed retreat strategies to reduce settlement expansion into high-risk erosion corridors(Michele et al., 2017).

REFERENCES

Caesar, J., Janes, T., Lindsay, A., & Bhaskaran, B. (2015). Temperature and precipitation projections over Bangladesh and the upstream Ganges, Brahmaputra and Meghna systems. Environmental Science: Processes and Impacts, 17(6), 1047–1056. https://doi.org/10.1039/c4em00650j

Community Report:Bhola. (n.d.).

Feyisa, G. L., Meilby, H., Fensholt, R., & Proud, S. R. (2014). Automated Water Extraction Index: A new technique for surface water mapping using Landsat imagery. Remote Sensing of Environment, 140, 23–35. https://doi.org/10.1016/J.RSE.2013.08.029

Gijón Mancheño, A., Jafino, B. A., Hofland, B., van Wesenbeeck, B. K., Kazi, S., & Urrutia, I. (2025a). Nature Meets Infrastructure: The Role of Mangroves in Strengthening Bangladesh's Coastal Flood Defenses. Sustainability 2025, Vol. 17, Page 1567, 17(4), 1567. https://doi.org/10.3390/SU17041567

Mahmood, R., Zhang, L., & Li, G. (2023). Assessing effectiveness of nature-based solution with big earth data: 60 years mangrove plantation program in Bangladesh coast. Ecological Processes, 12(1). https://doi.org/10.1186/s13717-023-00419-y

McFeeters, S. K. (1996). The use of the Normalized Difference Water Index (NDWI) in the delineation of open water features. International Journal of Remote Sensing, 17(7), 1425–1432. https://doi.org/10.1080/01431169608948714

Rawal, S. (2022). Overcoming Path Dependency to Implement Nature-Based Solutions for Coastal Flooding: Cases from the Global North and South.

Xu, H. (2006). Modification of normalised difference water index (NDWI) to enhance open water features in remotely sensed imagery. International Journal of Remote Sensing, 27(14), 3025–3033. https://doi.org/10.1080/01431160600589179;PAGE:STRING:ARTICLE/CHAPTER

Ahmed, A., Nawaz, R., Drake, F., & Woulds, C. (2018). Modelling land susceptibility to erosion in the coastal area of Bangladesh: A geospatial approach. *Geomorphology*, *320*, 82–97. https://doi.org/10.1016/j.geomorph.2018.08.004

Almarshed, B., Figlus, J., Miller, J., & Verhagen, H. J. (2020). Innovative Coastal Risk Reduction through Hybrid Design: Combining Sand Cover and Structural Defenses. In *Journal of Coastal Research* (Vol. 36, Issue 1, pp. 174–188). Coastal Education Research Foundation Inc. https://doi.org/10.2112/JCOASTRES-D-18-00078.1

Anwar, M. S., & Rahman, K. (2021). The spatiotemporal shore morphological changes at east Bhola Island in Meghna Estuary of Bangladesh's central coast. *Regional Studies in Marine Science*, *47*. https://doi.org/10.1016/j.rsma.2021.101937

Bennett, M. (2021). *Using the Digital Shoreline Analysis System (DSAS) to Analyze Changes in Shoreline Position Caused by Seawalls Along a Section of Oregon's Coast Dedication*.

Biswas, A., & Islam, R. (2017). Coastal Erosion and Accretion on the Island of Bhola, Bangladesh. In *BIAM Foundation* (Vol. 63).

Daud, S., Milow, P., & Zakaria, R. M. (2021a). Analysis of Shoreline Change Trends and Adaptation of Selangor Coastline, Using Landsat Satellite Data. *Journal of the Indian Society of Remote Sensing*, *49*(8), 1869–1878. https://doi.org/10.1007/s12524-020-01218-0

Durap, A., & Balas, C. E. (2024). Towards sustainable coastal management: a hybrid model for vulnerability and risk assessment. *Journal of Coastal Conservation*, *28*(4). https://doi.org/10.1007/s11852-024-01065-y

Elahi, W. E. (n.d.). *River-tide interaction and cyclone-induced storm surge in the Ganges-Brahmaputra-Meghna delta*. https://doi.org/10.26190/unsworks/1626

Galib, S. A., & Moniruzzaman, S. (2012). Morphological Behaviour of Bhola Island and Its Associated Erosional and Depositional Features: A Remote Sensing and GIS Based Study. In *Journal of the Bangladesh National Geographical Association* (Vol. 40, Issue 2).

Golam, M., Sarwar, M., Supervisor, ☼, & Wallman, P. (n.d.). *Impacts of Sea Level Rise on the Coastal Zone of Bangladesh Masters thesis of*.

Islam, M. A., Hossain, M. S., & Murshed, S. (2015). Assessment of Coastal Vulnerability Due to Sea Level Change at Bhola Island, Bangladesh: Using Geospatial Techniques. *Journal of the Indian Society of Remote Sensing*, *43*(3), 625–637. https://doi.org/10.1007/s12524-014-0426-0

Manurung, R. F. P., Khakhim, N., & Susilo, B. (2025a). Quantify Relation of SLR and Changes Along Karawang Coastal: GIS and Statistical Model Utilization. *IOP Conference Series: Earth and Environmental Science*, *1503*(1). https://doi.org/10.1088/1755-1315/1503/1/012030

Michele, G., Giovanni, M., Annibale, G., Lucia, T., Vito, S., & Angela, L. (2017). Development of an Integrated SDSS for Coastal Risks Monitoring and Assessment. *Journal of Coastal Zone Management*, *20*(3). https://doi.org/10.4172/2473-3350.1000446

Rahman, M., Akhand, R., & Uddin, H. (n.d.). *Remote Sensing and GIS Technology for Monitoring Bhola Island of Bangladesh*. www.theinternationaljournal.org

Tanvir Hassan, S. M., Mamnun Alfred Wegener, N., Abu Syed, M., & Mamnun, N. (2017). *Estimating erosion and accretion in the coast of Ganges-Brahmaputra-Meghna delta in Bangladesh*. https://www.researchgate.net/publication/315647843

Toledo, I., Pagán, J. I., Aragonés, L., & Crespo, M. B. (2024). Doing nothing is no solution: Coastal erosion management in Guardamar del Segura (Spain). *Marine Policy*, *169*. https://doi.org/10.1016/j.marpol.2024.106340

Uddin, M. J., Niloy, M. N. R., Haque, M. N., & Fayshal, M. A. (2023). Assessing the shoreline dynamics on Kuakata, coastal area of Bangladesh: a GIS- and RS-based approach. *Arab Gulf Journal of Scientific Research*, *41*(3), 240–259. https://doi.org/10.1108/AGJSR-07-2022-0114